IJST, Transactions of Mechanical Engineering, Vol. 38, No. M1, pp 25-44
Printed in The Islamic Republic of Iran, 2014

A COMBINATION OF PSEUDO-SPECTRAL METHOD AND EXTRAPOLATION FOR SOLVING MHD FLOW AND HEAT TRANSFER ABOUT A ROTATING DISK*

M. HEYDARI[1], G. B. LOGHMANI[2**] AND A. A. DEHGHAN[3]

[1,2]Dept. of Mathematics, Yazd University, Yazd, I. R. of Iran
Email: loghmani@yazd.ac.ir
[3]School of Mechanical Engineering, Yazd University, Yazd, I. R. of Iran

Abstract– The objective of this study is to implement a numerical method which is a combination of pseudo-spectral collocation method with a positive scaling factor and extrapolation for solving steady, laminar, incompressible, viscous and electrically conducting fluid of the boundary layer flow due to a constant temperature rotating disk subjected to a uniform suction and injection through its surface in the presence of a uniform transverse magnetic field. These equations are obtained from the Navier Stokes equations through the similarity transformations introduced by Von Karman in 1921. The proposed solution is equipped by the Chebyshev polynomials that have perfect properties to achieve this goal. This method solves the problem on the semi-infinite domain without truncating it to a finite domain. In addition, the presented method reduces solution of the problem to solution of a system of algebraic equations. The obtained numerical solutions are verified by the previous results in the literature.

Keywords– Navier stokes equations, MHD flow, rotating disk, suction and injection, Chebyshev polynomials, pseudo-spectral method, extrapolation, scaling factor

1. INTRODUCTION

Nonlinear phenomena, which appear in many areas of scientific fields such as solid state physics, plasma physics, fluid dynamics, mathematical biology and chemical kinetics, can be modeled by nonlinear ordinary or partial differential equations. Difficulty of solving the nonlinear problems or obtaining an analytic solution, leads to the use of numerical methods. Nowadays, there are several methods that can be used to obtain these numerical or analytically approximate solutions. These known methods are, for example, Euler method, Runge-Kutta method, multi-step method, Taylor series method, Hybrid methods, family of finite difference methods [1, 2], meshless methods, differential quadrature, spectral methods [3-8] to name a few. Furthermore, there are other methods which give analytically approximate solutions like family of finite element methods [9], the δ-expansion method [10], the artificial small parameter method [11], perturbation methods [12, 13], the Adomian decomposition method [14], the variational iteration method [15, 16], the homotopy perturbation method [17, 18] and the homotopy analysis method [19, 20].

The spectral methods arise from the fundamental problem of approximation of a function by interpolation on an interval, and are very powerful tools for solving many types of differential equations in various fields of science and engineering [8, 21]. The basic idea of spectral methods to solve differential equations is to expand the solution function as a finite series of very smooth basis functions, as given

$$u^N(\xi) = \sum_{n=0}^{N} u_n \psi_n(\xi)$$

*Received by the editors December 12, 2012; Accepted July 21, 2013.
**Corresponding author

in which, the best choice of $\psi_n(\xi)$ are the eigenfunctions of a singular Sturm-Liouville problem.

The utility of these methods is based on the fact that if the solution sought is smooth, usually only a few terms in an expansion of global basis functions are needed to represent it to high degree of accuracy. This efficiency arises due to the nature of spectral coefficients,u_n, which tend to zero faster than any negative algebraic power of their index n, showing either exponential or sometimes super-exponential convergence [22].

The rotating disk flow is one of the classical and important problems in fluid mechanics. The rotating disk flows have practical applications in many areas, such as helicopter rotor aerodynamics [23, 24], chemical engineering [25], dynamic models [26], magnetic energy propulsion systems, lubrication, oceanography and computer storage devices. The fluid flow due to an infinite rotating disk was first considered by von Karman in 1921 [27]. He gave a formulation of the problem and then introduced his transformations which reduced the governing partial differential equations to ordinary differential equations. He also obtained an approximate solution for the problem by using an approximate integral method.

a) Literature review

Different techniques have been used to obtain analytical and numerical solutions for rotating disk equations.

Cochran [28] obtained a more accurate solution to the same problem by developing two expansions, a Taylor series expansion near the disk and a series solution involving exponentially decaying functions at a far distance from the disk and eventually matching the two in some intermediate region. The problem of heat transfer from a rotating disk at a constant temperature was first considered by Millsaps and Pohlhausen [29] for the values of Prandtl number (Pr) between 0.5 and 1.0. Stuart [30] obtained a series solution for uniform suction on the flow due to a rotating disk. His solution was obtained by integrating the differential equations away from the disk and matching the asymptotic boundary conditions at infinity. Sparrow and Gregg [31] developed numerical solutions for the steady state heat transfer from a rotating disk maintained at a constant temperature for a range of $0.1 < Pr < 100$ by neglecting the dissipative terms in the energy equation. Benton [32] improved the steady state solutions given by Cochran [28] and extended the problem to the unsteady state.

The effect of strong injection on the flow induced by the rotating disk was studied by Kuiken [33]. Ackroyd [34] showed that the expansion of Cochran is valid for large distances from the disk and can actually be extended all the way to the disk. Numerical solutions of the MHD flow near a rotating disk for a wide range of imposed magnetic field strengths and injection and suction velocities based on modern quasi-Newton and globally convergent homotopy methods have been given by Kumar et al. [35]. Ariel in [36] presented an exponentially-decaying solution idea of [34] for the nonconducting fluid flow case to the conducting fluid flow of the rotating disk boundary layer. Ariel's series solution, numerically computed the velocity profiles for any value of the magnetic interaction parameter, but the effects of suction or blowing through the wall were omitted. Turkyilmazoglu in [37, 38] used the homotopy analysis method to solve the equations governing the flow of a steady, laminar, incompressible, viscous, and electrically conducting fluid due to a rotating disk subjected to a uniform suction and injection through the walls in the presence of a uniform transverse magnetic field.

b) The main aim of the present method

In the present work, a combination of pseudo-spectral collocation method with a positive scaling factor and extrapolation is used to solve the MHD flow about a rotating disk subjected to a uniform suction and injection with heat transfer. The main point of the present analysis lies in the fact that the

present method solves the problem on the semi-infinite domain without truncating it to a finite domain. The results are compared with those in the literature [35-38] that include suction/injection and an applied magnetic field.

The outline of the paper is as follows: In section 2, the mathematical formulation is presented. Some necessary definitions and mathematical preliminaries of the Chebyshev polynomials are introduced in Section 3. In Section 4, a numerical method for solving MHD flow and heat transfer about a rotating disk is presented. Results and comparisons with existing methods in the literature are presented in Section 5 and finally conclusions are drawn in Section 6.

2. MATHEMATICAL FORMULATION

We set the disk in the plane $z = 0$ and the space $z > 0$ is filled by a homogeneous, incompressible, electrically conducting viscous fluid. A schematic diagram of the problem is shown in Fig. 1. Here (r, θ, z) are cylindrical coordinates, B_0 is the externally applied magnetic field in the z direction, ω is the angular velocity of the disk, T_w is the uniform temperature at the disk surface and T_∞ is the ambient fluid temperature. The equations of steady motion are as follows [31, 35]:

$$\frac{\partial}{\partial r}(ru) + \frac{\partial}{\partial z}(rw) = 0 \tag{1}$$

$$\rho\left[\left(u\frac{\partial}{\partial r} + w\frac{\partial}{\partial z}\right)u - \frac{v^2}{r}\right] = -\frac{\partial p}{\partial r} + \mu\left(\nabla^2 u - \frac{u}{r^2}\right) - \sigma B_0^2 u \tag{2}$$

$$\rho\left[\left(u\frac{\partial}{\partial r} + w\frac{\partial}{\partial z}\right)v + \frac{uv}{r}\right] = \mu\left(\nabla^2 v - \frac{v}{r^2}\right) - \sigma B_0^2 v \tag{3}$$

$$\rho\left[u\frac{\partial}{\partial r} + w\frac{\partial}{\partial z}\right]w = -\frac{\partial p}{\partial z} + \mu\nabla^2 w \tag{4}$$

where u, v and w are the velocity components in the r, θ, z directions respectively, ρ is the density of the fluid, μ is the coefficient of viscosity, p is the pressure and σ is the electrical conductivity. The boundary conditions are introduced as

$$u = 0, \quad v = r\omega, \quad w = -w_0, \quad at \quad z = 0 \tag{5}$$

$$u = 0, \quad v = 0, \quad p = 0, \quad at \quad z \to \infty \tag{6}$$

where $w_0 > 0$ corresponds to suction and $w_0 < 0$ corresponds to injection. Kumar et al. [35] introduced von Karman transformations as [27]

$$u = r\omega F(\eta),\ v = r\omega G(\eta),\ w = \sqrt{\omega\upsilon}H(\eta),\ \ p = -\rho\nu\omega P(\eta),\ \ \eta = \sqrt{\frac{\omega}{\nu}}z \tag{7}$$

where η is the independent similarity variable and represent a non-dimensional distance measured along the axis of rotation, F, G, H and P are non-dimensional functions of η and ν is the kinematic viscosity of the fluid, $\nu = \mu/\rho$ [27]. With these transformations, Eqs. (1)-(4) take the following forms:

$$\frac{dH}{d\eta} + 2F = 0 \tag{8}$$

$$\frac{d^2F}{d\eta^2} - H\frac{dF}{d\eta} - F^2 + G^2 - mF = 0 \tag{9}$$

$$\frac{d^2G}{d\eta^2} - H\frac{dG}{d\eta} - 2FG - mG = 0 \tag{10}$$

$$\frac{d^2H}{d\eta^2} - H\frac{dH}{d\eta} + \frac{dP}{d\eta} = 0 \tag{11}$$

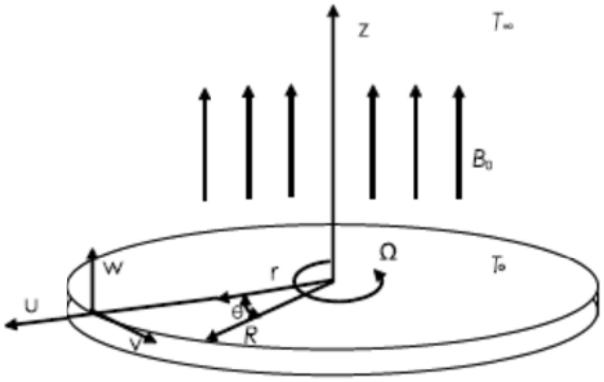

Fig. 1. Schematic diagram of the problem

subject to the boundary conditions

$$F(0) = 0, \quad G(0) = 1, \quad H(0) = -s \tag{12}$$

$$F(\infty) = 0, \quad G(\infty) = 0, \quad P(\infty) = 0 \tag{13}$$

where the primes denote differentiation with respect to η, $m = \sigma B_0^2/\rho\omega$ is the magnetic interaction number [39] and $s = w_0/\sqrt{\omega\nu}$ is the uniform injection (suction) parameter. $s > 0$ represents suction while $s < 0$ represents injection. Equation (12) indicates the no-slip condition of viscous flow on the disk. Furthermore, from the surface of the disk, all the non-dimensional fluid velocities except $H(\eta)$ must vanish aside the induced axial component as indicated in equation (13) [40]. Equation (11) can be used to compute the pressure distribution.

Due to the temperature difference between the wall and the ambient fluid, heat transfer takes place. The energy equation can be reduced to the following form [31, 41]

$$\rho c_p \left(u\frac{\partial T}{\partial r} + w\frac{\partial T}{\partial z}\right) - k\left(\frac{\partial^2 T}{\partial z^2} + \frac{\partial^2 T}{\partial r^2} + \frac{1}{r}\frac{\partial T}{\partial r}\right) = 0 \tag{14}$$

where T is the temperature of the fluid, c_p is the constant pressure specific heat of the fluid and k is the fluid thermal conductivity of the fluid. The boundary conditions for temperature are given by

$$T(0) = T_w, \quad T(\infty) = T_\infty \tag{15}$$

where T_w and T_∞ are the temperature of the surface of the disk and ambient temperature, respectively. The non-dimensional temperature variable Θ is introduced as follows:

$$\Theta(\eta) = \frac{T - T_\infty}{T_w - T_\infty} \tag{16}$$

The energy equation is reduced by using (7) and (16) in the form given below

$$\frac{1}{Pr}\frac{d^2\Theta}{d\eta^2} - H\frac{d\Theta}{d\eta} = 0 \tag{17}$$

where Pr is the Prandtl number, $Pr = c_p\mu/k$. The non-dimensional temperature boundary conditions are

$$\Theta(0) = 1, \quad \Theta(\infty) = 0 \tag{18}$$

The heat transfer from the disk surface to the fluid is computed by application of Fourier's law

$$q = -k\left(\frac{\partial T}{\partial z}\right)_w \tag{19}$$

Introducing the transformed variables, the expression for q becomes

$$q = -k(T_w - T_\infty)\sqrt{\frac{\omega}{\upsilon}}\Theta'(0) \tag{20}$$

The Nusselt number is given by

$$Nu = \frac{q}{k(T_w - T_\infty)}\sqrt{\frac{\upsilon}{\omega}} \tag{21}$$

So, from (20) and (21), we can get the Nusselt number as follows:

$$Nu = -\Theta'(0) \tag{22}$$

3. SOME PRELIMINARIES

a) Properties of Chebyshev polynomials

The well known Chebyshev polynomials of the first kind [6] of degree n are defined on the interval $[-1,1]$ as

$$T_n(\xi) = \cos(n\arccos(\xi)) \tag{23}$$

Obviously, $T_0(\xi) = 1, T_1(\xi) = \xi$ and they satisfy the recurrence relations:

$$T_{n+1}(\xi) = 2\xi T_n(\xi) - T_{n-1}(\xi), \quad n = 1,2,\cdots \tag{24}$$

Square integrable function $u(\xi)$ in $[-1,1]$, may be expressed in terms of Chebyshev polynomials as

$$u(\xi) = \sum_{j=0}^{\infty}{}' u_j T_j(\xi) \tag{25}$$

where the coefficients u_j are given by

$$u_j = \frac{(u(\xi),T_j(\xi))_w}{(T_j(\xi),T_j(\xi))_w}, \quad j = 0,1,2,\cdots \tag{26}$$

Here, $w(\xi) = \frac{1}{\sqrt{1-\xi^2}}$ and $(.,.)_w$ is the inner product of $L_w^2(-1,1)$. We choose the grid (interpolation) points to be the extrema

$$\xi_i = \cos\left(\frac{i\pi}{N}\right), \quad i = 0,1,\cdots,N \tag{27}$$

of the Nth order Chebyshev polynomial $T_N(\xi)$. These grids, $\xi_N = -1 < \xi_{N-1} < \cdots < \xi_1 < \xi_0 = 1$ are also viewed as the zeros of $(1-\xi^2)\frac{dT_N(\xi)}{d\xi}$. Clenshaw and Curtis [7] introduced the following approximation of the function u(ξ),

$$u^N(\xi) \simeq \sum_{j=0}^{N}{}'' \tilde{u}_j T_j(\xi) \tag{28}$$

where $\tilde{u}_j$ are the Chebyshev coefficients which are determined by the formulations

$$\tilde{u}_j = \frac{2}{N\tilde{c}_j}\sum_{i=0}^{N}{}'' \frac{1}{\tilde{c}_i} u(\xi_i)\cos\left(\frac{\pi ij}{N}\right), \quad j = 0,1,\cdots,N \tag{29}$$

and

$$\tilde{c}_j = \begin{cases} 2, & j = 0,N \\ 1, & 1 \le j \le N-1 \end{cases} \tag{30}$$

As it is well-known in Chebyshev pseudo-spectral method, derivatives of the functions u(ξ) at the collocation points are presented as

$$\frac{du}{d\xi}(\xi_i) = \sum_{j=0}^{N} \mathcal{D}_{ij} u(\xi_j) \tag{31}$$

$$\frac{d^2u}{d\xi^2}(\xi_i) = \sum_{j=0}^{N} \mathcal{D}_{ij}^{(2)} u(\xi_j) \tag{32}$$

In the above equations $\mathcal{D}$ is the Chebyshev differentiation matrix and $\mathrm{N}+1$ is the number of collocation points (nodes) and $\mathcal{D}^{(2)} = (\mathcal{D})^2$. The entries of the differentiation matrix $\mathcal{D}$ are given by [42]

$$\mathcal{D}_{ij} = \begin{cases} \frac{2N^2+1}{6}, & i = j = 0 \\ -\frac{2N^2+1}{6}, & i = j = N \\ -\frac{x_i}{2\sin^2\left(\frac{i\pi}{N}\right)}, & i = j \neq 0, N \\ -\frac{1}{2}\frac{\tilde{c}_i}{\tilde{c}_j}\frac{(-1)^{i+j}}{\sin\left(\frac{(i+j)\pi}{2N}\right)\sin\left(\frac{(i-j)\pi}{2N}\right)}, & i \neq j \end{cases} \tag{33}$$

b) Mappings [8, 42]

A common and effective method for solving differential equation with unbounded domain is to use a suitable mapping that transforms a problem with infinite domain to a problem with finite domain.

We consider a family of mappings as follows:

$$\eta = g(\xi; L), \quad \xi \in I = (-1,1), \quad \eta \in \Lambda = (0, +\infty) \tag{34}$$

such that

$$\frac{d\eta}{d\xi} = g'(\xi; L) > 0, \quad \xi \in I = (-1,1) \tag{35}$$

$$g(-1; L) = 0, \quad g(1; L) = +\infty \tag{36}$$

Here, the parameter L is a positive scaling factor that is called mapping parameter. Without loss of generality, we further assume that the mapping is explicitly invertible, and denote its inverse mapping by

$$\xi = g^{-1}(\eta; L) := h(\eta; L), \quad \eta \in \Lambda = (0, +\infty), \quad \xi \in I = (-1,1) \tag{37}$$

There are several typical mappings that relate infinite and finite domains to each other, but three specific types of mappings, as algebraic, logarithmic, and exponential, are more practical [43]. Boyd in [8, 44] offered guidelines for optimizing the map parameter L for rational Chebyshev functions, which is useful for the presented method in this paper, too. For a general mapping $\eta = g(\xi; L)$ with $g'(\xi; L) > 0, \xi \in I = (-1,1)$, the first and second derivatives of $U(\eta)$ can be expressed in terms of ξ as follows:

$$\frac{dU}{d\eta} = \left(\frac{dg(\xi;L)}{d\xi}\right)^{-1} \frac{dU}{d\xi} \tag{38}$$

$$\frac{d^2U}{d\eta^2} = \left(\frac{dg(\xi;L)}{d\xi}\right)^{-2} \frac{d^2U}{d\xi^2} - \left(\frac{d^2g(\xi;L)}{d\xi^2}\right)\left(\frac{dg(\xi;L)}{d\xi}\right)^{-3} \frac{dU}{d\xi} \tag{39}$$

4. THE METHOD OF SOLUTION

The present work deals with application of a combination of pseudo-spectral collocation method with a positive scaling factor and extrapolation for solving MHD flow and heat transfer about a rotating disk with suction and injection. This method solves the problem on the semi-infinite domain without truncating it to a finite domain. If semi-infinite domain $[0, +\infty)$ truncation to a domain $[0, \eta_\infty]$ is employed then η_∞ must

be chosen. If one knows the rate at which $U(\eta)$ decays for large η, η_∞ can be chosen so that $U(\eta_\infty) < \varepsilon$ where ε is some user-chosen tolerance. But then one is still faced with choosing the grid spacing h so that the error in solving the differential equation on interval $[0, \eta_\infty]$ is small. If h is small, the error in solving the problem may be very much less than ε, in which case η_∞ was a bad choice because the domain truncation error is dominant, and it would have been better to choose a larger η_∞. In this paper, the algebraic mapping $\xi = \frac{\eta - L}{\eta + L}$ for converting semi-infinite domain $[0, +\infty)$ into the computational domain $(-1,1)$ is used. For this algebraic mapping, the Eqs. (38) and (39) can be writen as follows:

$$\frac{dU}{d\eta} = \frac{1}{2L}(1-\xi)^2 \frac{dU}{d\xi} \tag{40}$$

$$\frac{d^2U}{d\eta^2} = \frac{1}{4L^2}(1-\xi)^4 \frac{d^2U}{d\xi^2} - \frac{1}{2L^2}(1-\xi)^3 \frac{dU}{d\xi} \tag{41}$$

By using (40) and (41), the Eqs. (8)-(10) are converted to the differential equations with boundary conditions on interval $[-1,1]$ as follows:

$$2F + \frac{1}{2L}(1-\xi)^2 \frac{dH}{d\xi} = 0 \tag{42}$$

$$\left[\frac{1}{4L^2}(1-\xi)^4 \frac{d^2F}{d\xi^2} - \frac{1}{2L^2}(1-\xi)^3 \frac{dF}{d\xi}\right] - \left[\frac{1}{2L}(1-\xi)^2 \frac{dF}{d\xi}\right] H - F^2 + G^2 - mF = 0 \tag{43}$$

$$\left[\frac{1}{4L^2}(1-\xi)^4 \frac{d^2G}{d\xi^2} - \frac{1}{2L^2}(1-\xi)^3 \frac{dG}{d\xi}\right] - \left[\frac{1}{2L}(1-\xi)^2 \frac{dG}{d\xi}\right] H - 2FG - mG = 0 \tag{44}$$

and

$$F(-1) = 0, \quad G(-1) = 1, \quad H(-1) = -s \tag{45}$$

$$F(1) = 0, \quad G(1) = 0 \tag{46}$$

Now, we apply Chebyshev pseudo-spectral method to solve the above problem as follows. This method involves using the Chebyshev-Gauss-Lobatto points (27) to discrete interval $[-1,1]$. Consider the unknown functions $F(\xi), G(\xi)$ and $H(\xi)$ which can be approximated as a truncated series of Chebyshev polynomials

$$F(\xi) \simeq F^N(\xi) = \sum_{j=0}^{N} \tilde{f}_j T_j(\xi) \tag{47}$$

$$G(\xi) \simeq G^N(\xi) = \sum_{j=0}^{N} \tilde{g}_j T_j(\xi) \tag{48}$$

$$H(\xi) \simeq H^N(\xi) = \sum_{j=0}^{N} \tilde{h}_j T_j(\xi) \tag{49}$$

where $\tilde{f}_j, \tilde{g}_j$ and $\tilde{h}_j$ are the Chebyshev coefficients which are determined by the formulations

$$\tilde{f}_j = \frac{2}{N\tilde{c}_j} \sum_{i=0}^{N} \frac{1}{\tilde{c}_i} F(\xi_i) \cos\left(\frac{\pi i j}{N}\right), \quad j = 0,1,\cdots,N \tag{50}$$

$$\tilde{g}_j = \frac{2}{N\tilde{c}_j} \sum_{i=0}^{N} \frac{1}{\tilde{c}_i} G(\xi_i) \cos\left(\frac{\pi i j}{N}\right), \quad j = 0,1,\cdots,N \tag{51}$$

$$\tilde{h}_j = \frac{2}{N\tilde{c}_j} \sum_{i=0}^{N} \frac{1}{\tilde{c}_i} H(\xi_i) \cos\left(\frac{\pi i j}{N}\right), \quad j = 0,1,\cdots,N \tag{52}$$

By employing derivatives formulations (31) and (32), Eqs. (42)-(46) are transformed to the following expressions

$$2F(\xi_i) + \frac{1}{2L}(1-\xi_i)^2 \sum_{j=0}^{N} \mathcal{D}_{ij} H(\xi_j) = 0 \tag{53}$$

$$\left[\frac{1}{4L^2}(1-\xi_i)^4\sum_{j=0}^{N}\mathcal{D}_{ij}^{(2)}F(\xi_j)-\frac{1}{2L^2}(1-\xi_i)^3\sum_{j=0}^{N}\mathcal{D}_{ij}F(\xi_j)\right]$$
$$-\left[\frac{1}{2L}(1-\xi_i)^2\sum_{j=0}^{N}\mathcal{D}_{ij}F(\xi_j)\right]H(\xi_i)-[F(\xi_i)]^2+[G(\xi_i)]^2-mF(\xi_i)=0 \quad (54)$$

$$\left[\frac{1}{4L^2}(1-\xi_i)^4\sum_{j=0}^{N}\mathcal{D}_{ij}^{(2)}G(\xi_j)-\frac{1}{2L^2}(1-\xi_i)^3\sum_{j=0}^{N}\mathcal{D}_{ij}G(\xi_j)\right]$$
$$-\left[\frac{1}{2L}(1-\xi_i)^2\sum_{j=0}^{N}\mathcal{D}_{ij}G(\xi_j)\right]H(\xi_i)-2F(\xi_i)G(\xi_i)-mG(\xi_i)=0 \quad (55)$$

where $i=1,2,\cdots,N-1$ and

$$F(\xi_N)=0,\quad G(\xi_N)=1,\quad H(\xi_N)=-s \quad (56)$$

$$F(\xi_0)=0,\quad G(\xi_0)=0 \quad (57)$$

For finding approximate solutions $F(\xi),G(\xi)$ and $H(\xi)$, the values $\{F(\xi_i)\}_{i=1}^{N-1},\{G(\xi_i)\}_{i=1}^{N-1}$ and $\{H(\xi_i)\}_{i=0}^{N-1}$ must be calculated. But, the equations (53)-(55) give a system with $3N-3$ equations and $3N-2$ unknowns. To construct the remaining one equation, extrapolation method can be used. Extrapolating is defined as estimating a point outside a known data set. Here, we consider N data points $\{(\xi_i,H(\xi_i))\}_{i=1}^{N}$ generated by the unknown function $H(\xi)$. So, we can interpolate H(ξ) by the Lagrange form of the interpolation polynomial as follows:

$$H(\xi)\simeq\sum_{j=1}^{N}H(\xi_j)L_j(\xi) \quad (58)$$

where

$$L_j(\xi)=\prod_{k=1,k\neq j}^{N}\frac{\xi-\xi_k}{\xi_j-\xi_k},\quad j=1,2,\cdots,N \quad (59)$$

are Lagrange polynomials. By collocating (58) in point ξ_0, we obtain

$$H(\xi_0)-\sum_{j=1}^{N}H(\xi_j)L_j(\xi_0)=0 \quad (60)$$

Equations (53)-(55) together with Eq. (60) give a $(3N-2)\times(3N-2)$ system of nonlinear equations, which can be solved for $\{F(\xi_i)\}_{i=1}^{N-1},\{G(\xi_i)\}_{i=1}^{N-1}$ and $\{H(\xi_i)\}_{i=0}^{N-1}$, using Newton's iterative method [44, 45]. After evaluating $F(\xi),G(\xi)$ and $H(\xi)$, the original functions $F(\eta),G(\eta)$ and $H(\eta)$ are obtained as follows:

$$F(\eta)\simeq F^N(\eta)=\sum_{j=0}^{N}\tilde{f}_jT_j\left(\frac{\eta-L}{\eta+L}\right) \quad (61)$$

$$G(\eta)\simeq G^N(\eta)=\sum_{j=0}^{N}\tilde{g}_jT_j\left(\frac{\eta-L}{\eta+L}\right) \quad (62)$$

$$H(\eta)\simeq H^N(\eta)=\sum_{j=0}^{N}\tilde{h}_jT_j\left(\frac{\eta-L}{\eta+L}\right) \quad (63)$$

Now, by using approximate solution (63) for function $H(\eta)$, we apply a similar method based on pseudo-spectral method for solving equation (17). By using (40) and (41), the equations (17) and (18) are converted to the differential equations as follows:

$$\frac{1}{Pr}\left[\frac{1}{4L^2}(1-\xi)^4\frac{d^2\Theta}{d\xi^2}-\frac{1}{2L^2}(1-\xi)^3\frac{d\Theta}{d\xi}\right]-\left[\frac{1}{2L}(1-\xi)^2\frac{d\Theta}{d\xi}\right]H\left(L\frac{1+\xi}{1-\xi}\right)=0 \quad (64)$$

$$\Theta(-1)=1,\quad \Theta(1)=0 \quad (65)$$

Consider the unknown function $\Theta(\xi)$ can be approximated as a truncated series of Chebyshev polynomials

$$\Theta(\xi) \simeq \Theta^N(\xi) = \sum_{j=0}^{N} \tilde{\theta}_j T_j(\xi) \tag{66}$$

where

$$\tilde{\theta}_j = \frac{2}{N\tilde{c}_j} \sum_{i=0}^{N} \frac{1}{\tilde{c}_i} \Theta(\xi_i) \cos\left(\frac{\pi i j}{N}\right), \qquad j = 0,1,\cdots,N \tag{67}$$

By employing derivatives formulations (31) and (32), Eqs. (64) and (65) are transformed to the following expressions:

$$\frac{1}{Pr}\left[\frac{1}{4L^2}(1-\xi_i)^4 \sum_{j=0}^{N} \mathcal{D}_{ij}^{(2)} \Theta(\xi_j) - \frac{1}{2L^2}(1-\xi_i)^3 \sum_{j=0}^{N} \mathcal{D}_{ij} \Theta(\xi_j)\right]$$

$$-\left[\frac{1}{2L}(1-\xi_i)^2 \sum_{j=0}^{N} \mathcal{D}_{ij} \Theta(\xi_j)\right] H\left(L\frac{1+\xi_i}{1-\xi_i}\right) = 0, \qquad i = 1,2,\cdots,N-1 \tag{68}$$

$$\Theta(\xi_N) = 1, \qquad \Theta(\xi_0) = 0 \tag{69}$$

Equations (68) give a $(N-1)\times(N-1)$ system of linear equations, which can be solved for $\{\Theta(\xi_i)\}_{i=1}^{N-1}$, using Newton's iterative method and we obtain

$$\Theta(\eta) \simeq \Theta^N(\eta) = \sum_{j=0}^{N} \tilde{\theta}_j T_j\left(\frac{\eta - L}{\eta + L}\right) \tag{70}$$

Remark 4.1 *The values of* $F'(0), G'(0), H(\infty)$ *and* $Nu = -\Theta'(0)$ *can be obtained from (61)-(63) and (70) as follows:*

$$F'(0) \simeq \frac{2}{L} \sum_{j=0}^{N} (-1)^{j+1} j^2 \tilde{f}_j \tag{71}$$

$$G'(0) \simeq \frac{2}{L} \sum_{j=0}^{N} (-1)^{j+1} j^2 \tilde{g}_j \tag{72}$$

$$H(\infty) \simeq \sum_{j=0}^{N} \tilde{h}_j \tag{73}$$

and

$$Nu = -\Theta'(0) \simeq \frac{2}{L} \sum_{j=0}^{N} (-1)^{j} j^2 \tilde{\theta}_j \tag{74}$$

We note that $T_n(\pm 1) = (\pm 1)^n$ *and* $T'_n(\pm 1) = (\pm 1)^{n+1} n^2$. *Furthermore, the value of* c *in Ariel's series solution [36] can be obtained by solving the nonlinear equation*

$$c^2 + \left[\sum_{j=0}^{N} \tilde{h}_j\right] c - m = 0 \tag{75}$$

5. RESULTS AND DISCUSSION

In this section we present the numerical and graphical results obtained from pseudo-spectral collocation method applied to the above problem. This section describes the influence of some governing parameters on the velocity and temperature fields. In particular, attention has been focused on the variations of the magnetic interaction number m, uniform injection (suction) parameter s and the Prandtl number Pr on the velocity and temperature fields, respectively. The current results are compared with the previously published results by Kumar et al. [35], Pande [47], Ariel [36] and Turkyilmazoglu [37, 38]. The computations were performed using MAPLE 13 with a Personal Computer. Intel Core 2 Duo processor with 4 GB RAM is used for the computation.

Figures 2-4 show the normalized velocity profiles $F(\eta), G(\eta)$ and $H(\eta)$ obtained by the presented method with $N = 30$ and scaling factor $L = 5$ in comparison to the numerical solution by the fourth-order

Runge-Kutta method and shooting method. It is seen from Fig. 2a that increasing the injection parameter (higher negative values of s) will result in higher radial velocities due to the mass flow injected. However, due to thickening the boundary layer, the injection process will result in a lower heat transfer coefficient. Figs. 2b and 2c show that increasing the magnetic number m causes a weaker flow field in the radial direction and hence will oppose the induced flow towards the disk. Figure 3a shows that for specified values of magnetic number m, increasing the injection process (higher negative values of s) will result in stronger velocities in the radial direction, while increasing s towards more positive values (stronger suction) will result in a thinner boundary layer thickness. Figures 3b and 3c show that for both suction and injection process (all values of s), increasing the magnetic number m will result in a weaker flow field in the radial direction. Regarding the inward flow velocity ($H(\eta)$), it is seen in Fig. 4a that increasing suction flow rate (more positive values of s) results in a higher inward flow towards the disk. This effect is the same as decreasing the magnetic field strength or m, as may be seen in Figs. 4a and 4b.

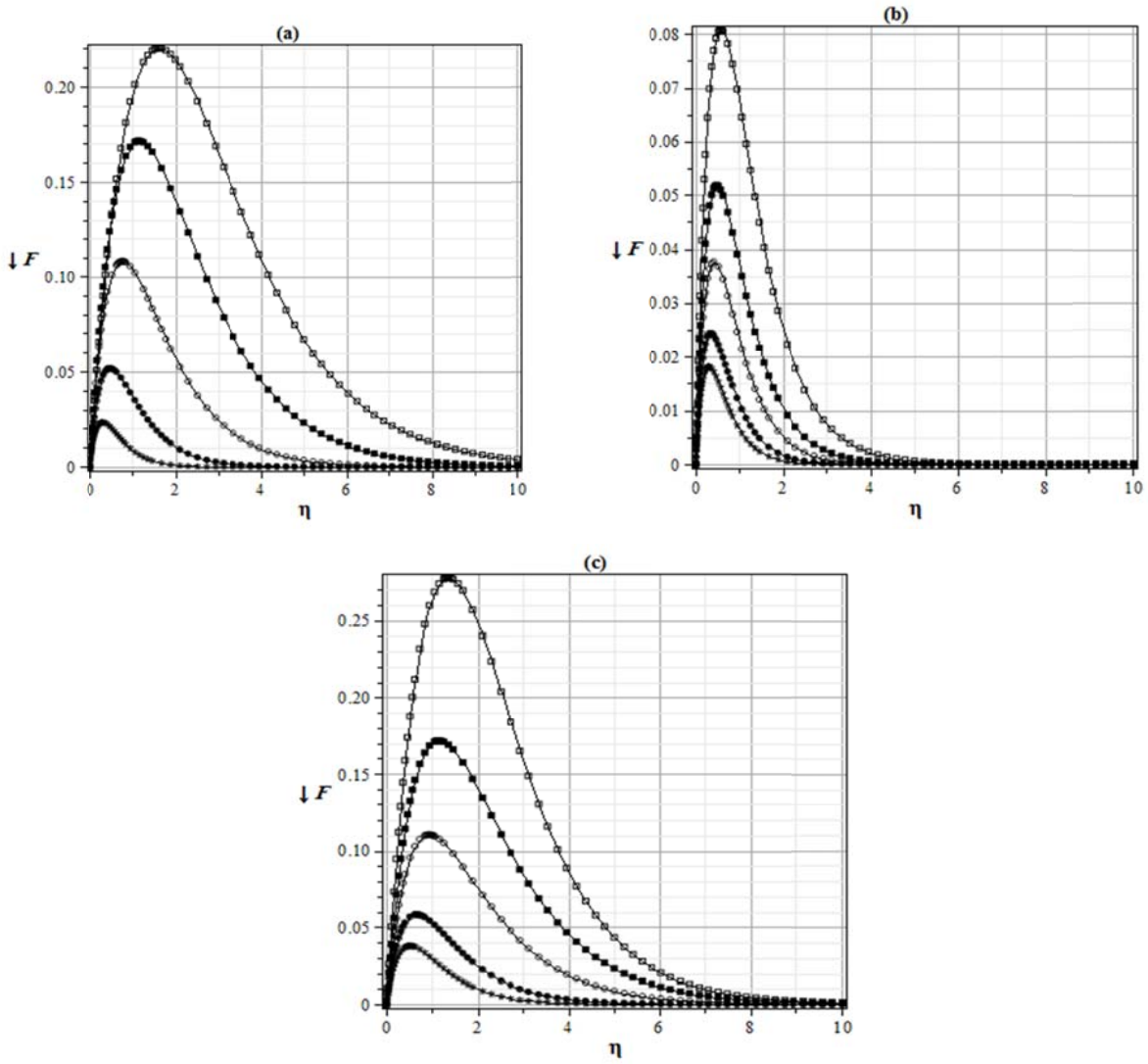

Fig. 2. Radial velocity $F(\eta)$. (a) Effect of s, $m = 0.5$, for $s = -2$ (box), $s = -1$ (solid-box), $s = 0$ (circle), $s = 1$ (solid-circle) and $s = 2$ (asterisk) in comparison to the numerical solution (line). (b) Effect of m, $s = 1$, for $m = 0$ (box), $m = 0.5$ (solid-box), $m = 1$ (circle), $m = 2$ (solid-circle) and $m = 3$ (asterisk) in comparison to the numerical solution (line). (c) Effect of m, $s = -1$, for $m = 0$ (box), $m = 0.5$ (solid-box), $m = 1$ (circle), $m = 2$ (solid-circle) and $m = 3$ (asterisk) in comparison to the numerical solution (line)

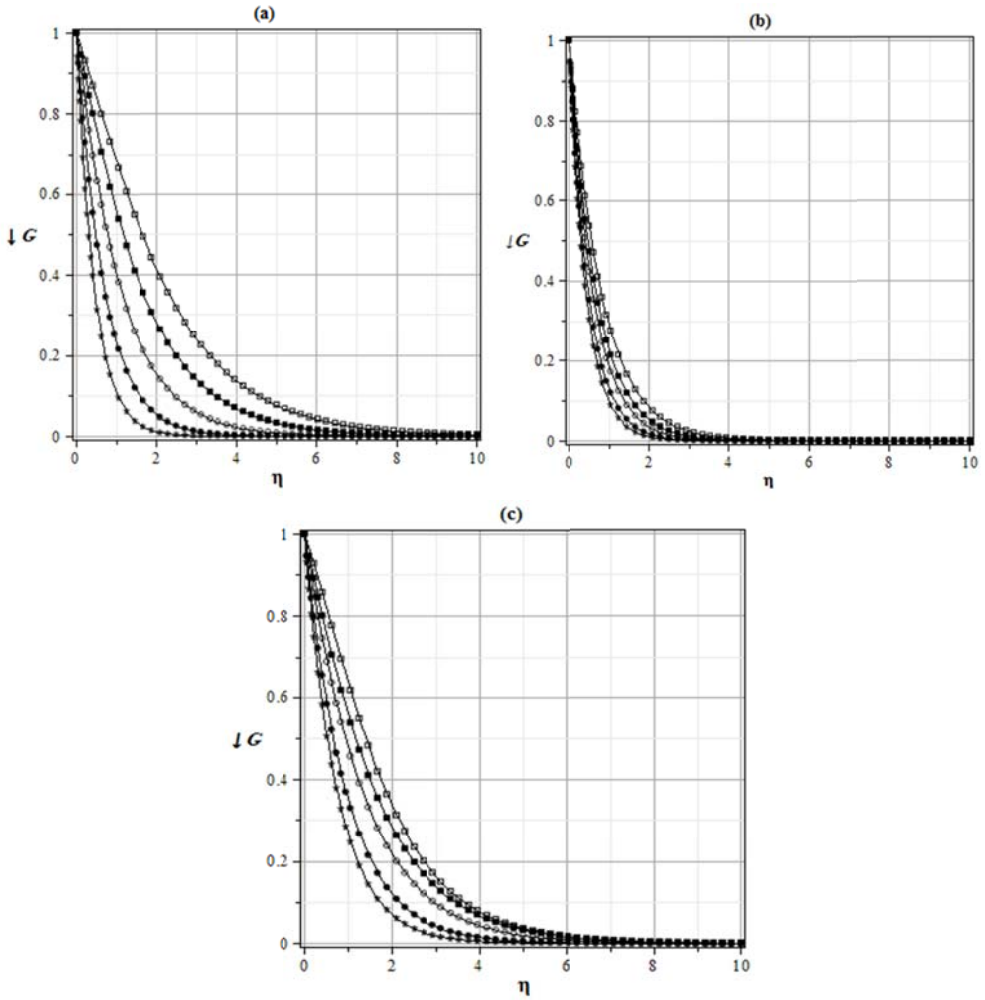

Fig. 3. Tangential velocity G(η). (a) Effect of s, m = 0.5, for s = −2 (box), s = −1 (solid-box), s = 0 (circle), s = 1 (solid-circle) and s = 2 (asterisk) in comparison to the numerical solution (line). (b) Effect of m, s = 1, for m = 0 (box), m = 0.5 (solid-box), m = 1 (circle), m = 2 (solid-circle) and m = 3 (asterisk) in comparison to the numerical solution (line). (c) Effect of m, s = −1, for m = 0 (box), m = 0.5 (solid-box), m = 1 (circle), m = 2 (solid-circle) and m = 3 (asterisk) in comparison to the numerical solution (line)

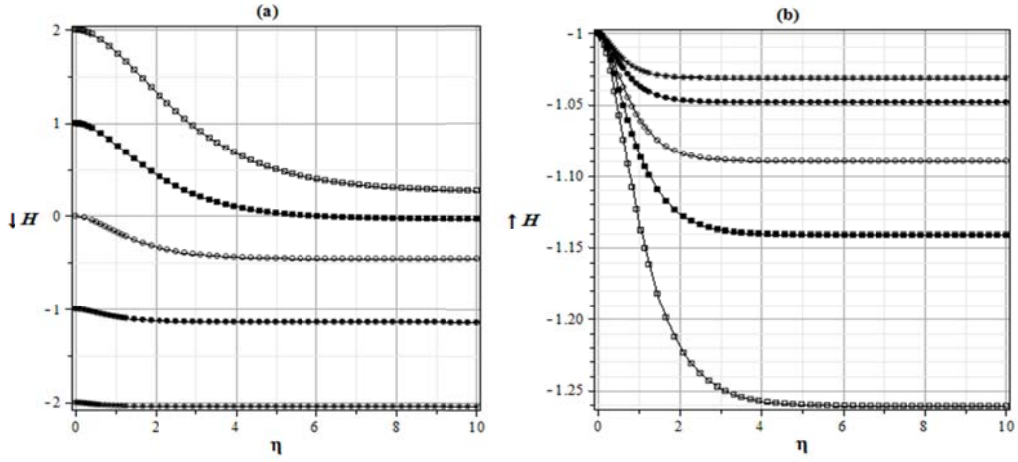

Fig. 4. Axial velocity H(η). (a) Effect of s, m = 0.5, for s = −2 (box), s = −1 (solid-box), s = 0 (circle), s = 1 (solid-circle) and s = 2 (asterisk) in comparison to the numerical solution (line). (b) Effect of m, s = 1, for m = 0 (box), m = 0.5 (solid-box), m = 1 (circle), m = 2 (solid-circle) and m = 3 (asterisk) in comparison to the numerical solution (line). (c) Effect of m, s = −1, for m = 0 (box), m = 0.5 (solid-box), m = 1 (circle), m = 2 (solid-circle) and m = 3 (asterisk) in comparison to the numerical solution (line)

Figure 4 Continued.

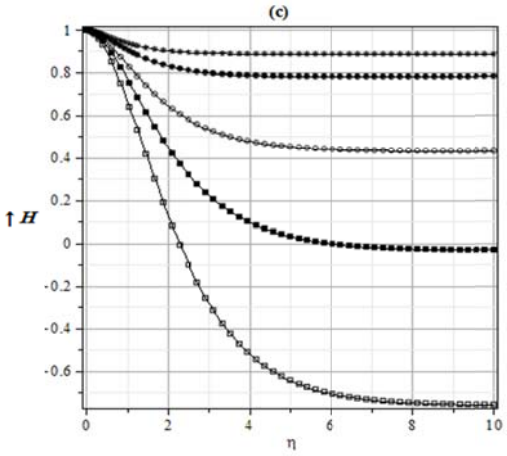

Tables 1 and 2 give a comparison between the presented method (PM) (with $N = 30$ and scaling factor $L = 3$) and the results reported by Turkyilmazoglu [37] for several suction/injection velocities. Here, by using (75) we can obtain the positive scaling factor c in Ariel's series solution.

Table 1. Comparison of the analytic solution of Turkyilmazoglu [37] and the present numerical results for $m = 1$

s	$F'(0)$ [37]	$F'(0)$(PM)	$G'(0)$ [37]	$G'(0)$(PM)	c [37]	c (PM)
-2.0	0.29148086	0.2914808631	-0.46571471	-0.4657148441	0.61611759	0.6161175910
-1.0	0.32166220	0.3216622168	-0.69066292	-0.6906628842	0.80719879	0.8071987873
0.0	0.30925798	0.3092579802	-1.06905336	-1.0690533599	1.13464624	1.1346462388
1.0	0.25104397	0.2510439720	-1.65707588	-1.6570758005	1.68373044	1.6837304442
2.0	0.18871903	0.1887190245	-2.43136154	-2.4313615383	2.44138137	2.4413813727

Table 2. Comparison of the analytic solution of Turkyilmazoglu [37] and the present numerical results for $m = 4$

s	$F'(0)$[37]	$F'(0)$(PM)	$G'(0)$ [37]	$G'(0)$(PM)	c [37]	c (PM)
-2.0	0.17398900	0.1739890031	-1.24715517	-1.2471551657	1.26701084	1.2670108401
-1.0	0.17467999	0.1746799901	-1.57312231	-1.5731223150	1.58828747	1.5882874718
0.0	0.16570305	0.1657030483	-2.01026672	-2.0102667198	2.02049160	2.0204915967
1.0	0.14901611	0.1490161140	-2.56932504	-2.5693250446	2.57556808	2.5755680776
2.0	0.12943847	0.1294384707	-3.24133921	-3.2413392135	3.24497851	3.2449785121

For some chosen values of magnetic strength parameter m, Table 3 gives a comparison between the presented method (PM) (with $N = 30$ and scaling factor $L = 3.5$) and the results reported by Turkyilmazoglu [36]. It is seen from Tables 1-3 that the maximum percentage of the absolute errors between the presented method and the analytic solution of Turkyilmazoglu [37] is $1.34 \times 10^{-5}\%$, $5.00 \times 10^{-9}\%$ and $1.54 \times 10^{-5}\%$, respectively.

Table 3. Comparison of the analytic solution of Turkyilmazoglu [37] and the present numerical results for $s = 0$

m	$F'(0)$[37]	$F'(0)$(PM)	$G'(0)$ [37]	$G'(0)$(PM)	c [37]	c (PM)
0	0.51023262	0.5102326127	-0.61592201	-0.6159220219	0.88447411	0.8844742638
1	0.30925798	0.3092579816	-1.06905336	-1.0690533552	1.13464624	1.1346462391
4	0.16570305	0.1657030483	-2.01026672	-2.0102667204	2.02049159	2.0204915968
25	0.06665659	0.0666565980	-5.00066641	-5.0006664150	5.00133276	5.0013327589
100	0.03333302	0.0333330172	-10.0000833	-10.000083336	10.0001667	10.000166662

In Tables 4 through 6, the values of $F'(0), -G'(0)$ and $-H(\infty)$ are presented for various m using Ariel's series solution (Section 3 [36]), perturbation solution for small m (Section 4 [36]), asymptotic solution for large m (Section 5 [36]), approximate solution for all m (Section 6 [36]) and the presented method with $s = 0, N = 25$ and scaling factor $L = 2.5$. It is observed from Tables 4-6 that the maximum percentage of the absolute errors between the presented method and the Ariel's series solution [36] is $4.93 \times 10^{-5}\%$, $5.44 \times 10^{-5}\%$ and $4.89 \times 10^{-2}\%$, and these absolute errors between the presented method and the approximate solution [36] are 1.39%, 2.19% and 4.96%, respectively.

Table 4. Variation of $F'(0)$ with magnetic parameter m for s = 0

m	Ariel [36]	Perturbation [36]	Asymptotic[36]	Approximate [36]	Presented method
0	0.510233	0.510233	− − − −	0.524131	0.5102325341
0.2	0.453141	0.453073	− − − −	0.459835	0.4531409669
0.4	0.405576	0.405383	− − − −	0.408736	0.4055757617
0.6	0.366698	0.367162	0.423279	0.368217	0.3666980939
0.8	0.335090	0.338411	0.346685	0.335851	0.3350897646
1.0	0.309258	0.319129	0.312477	0.309660	0.3092580035
1.2	0.287915	0.309316	0.289011	0.288239	0.2879153403
1.4	0.270049	0.308973	0.270481	0.270180	0.2700489432
1.6	0.254892	0.318099	0.255083	0.254973	0.2548923744
1.8	0.241872	0.336694	0.241964	0.241924	0.2418723429
2	0.230559	0.364759	0.230607	0.230593	0.2305591120
3	0.190503	− − − −	0.190509	0.190509	0.1905026514
5	0.148516	− − − −	0.148516	0.148516	0.1485155063
10	0.105310	− − − −	0.105310	0.105310	0.1053100366
20	0.074518	− − − −	0.074518	0.074518	0.0745180154
50	0.047139	− − − −	0.047139	0.047139	0.0471386715
100	0.033333	− − − −	0.033333	0.033333	0.0333330212

Table 5. Variation of $-G'(0)$ with magnetic parameter m for s = 0

m	Ariel [36]	Perturbation [36]	Asymptotic[36]	Approximate [36]	Presented method
0	0.615922	0.615922	− − − −	0.594064	0.6159219339
0.2	0.708795	0.709168	− − − −	0.695608	0.7087951858
0.4	0.802376	0.805456	− − − −	0.794648	0.8023761044
0.6	0.894476	0.904786	0.968507	0.889942	0.8944754840
0.8	0.983607	1.007159	0.995093	0.980887	0.9836069093
1.0	1.069053	1.112574	1.071620	1.067367	1.0690532935
1.2	1.150635	1.221031	1.151366	1.149551	1.1506349654
1.4	1.228466	1.332531	1.228714	1.227744	1.2284662495
1.6	1.302793	1.447073	1.302889	1.302296	1.3027935436
1.8	1.373906	1.564657	1.373947	1.373554	1.3739064040
2	1.442094	1.685284	1.442113	1.441837	1.4420940452
3	1.747686	− − − −	1.747686	1.747615	1.7476854843
5	2.243452	− − − −	2.243452	2.243440	2.2434522726
10	3.164907	− − − −	3.164907	3.164906	3.1649066944
20	4.473067	− − − −	4.473067	4.473067	4.4730670993
50	7.071303	− − − −	7.071303	7.071303	7.0713034924
100	10.000083	− − − −	10.000083	10.000083	10.000083337

The approximations of the $-H(\infty)$ obtained by Kumar et. al [35], asymptotic formula in [35] and the presented method with $N = 25$ and scaling factor $L = 9$ for some chosen values of Prandtl number (Pr) and magnetic interaction number m are listed in Table 7. From Table 7, we see that the asymptotic

formula does not have as much accuracy with injection values as it does for suction. It is shown from Table 7 that the maximum percentage of the absolute errors between the presented method and the obtained results in Kumar et. al [35] is $1.54 \times 10^{-1}\%$.

Table 6. Variation of $-H(\infty)$ with magnetic parameter m for $s = 0$

m	Ariel [36]	Perturbation [36]	Asymptotic[36]	Approximate [36]	Presented method
0	0.884474	0.884474	− − − −	0.835403	0.8849633172
0.2	0.683476	0.680910	− − − −	0.638026	0.6834764318
0.4	0.523397	0.507392	− − − −	0.489717	0.5233975704
0.6	0.403646	0.363923	− − − −	0.380936	0.4036456939
0.8	0.316535	0.250500	0.407199	0.301682	0.3165350930
1.0	0.253314	0.167125	0.273811	0.243576	0.2533142668
1.2	0.206874	0.113797	0.212757	0.200374	0.2068742244
1.4	0.172129	0.090517	0.174134	0.167684	0.1721286727
1.6	0.145605	− − − −	0.146384	0.142487	0.1456047656
1.8	0.124955	− − − −	0.125291	0.122714	0.1249554850
2	0.108584	− − − −	0.108740	0.106936	0.1085838042
3	0.061765	− − − −	0.061773	0.061299	0.0617654083
5	0.029402	− − − −	0.029402	0.029317	0.0294016556
10	0.010504	− − − −	0.010504	0.010496	0.0105039221
20	0.003723	− − − −	0.003723	0.003723	0.0037234972
50	0.000943	− − − −	0.000943	0.000943	0.0009426760
100	0.000333	− − − −	0.000333	0.000333	0.0003333216

Table 7. The comparison of $-H(\infty)$ for presented method, asymptotic formula and obtained results in Kumar et. al [35]

s	m	Asymptotic formula [35]	Kumar et. al [35]	Presented method
3	1	3.3333	3.0131	3.0131401
3	2	3.1178	3.0102	3.0101920
3	4	3.0417	3.0069	3.0069199
2	1	2.3333	2.0318	2.0317772
2	2	2.1178	2.0213	2.0212868
2	4	2.0417	2.0123	2.0123047
1	1	1.3333	1.0898	1.0898111
1	2	1.1178	1.0481	1.0481266
1	4	1.0417	1.0225	1.0225126
0	1	0.33333	0.25331	0.2533143
0	2	0.11785	0.10858	0.1085838
0	4	0.04172	0.04078	0.0407754
−1	1	−0.6667	−0.43166	−0.4316534
−1	2	−0.8822	−0.78157	−0.7815625
−1	4	−0.9583	−0.93015	−0.9301483
−2	1	−1.6667	−1.0070	−1.0069492
−2	2	−1.8822	−1.6265	−1.6264850
−2	4	−1.9583	−1.8900	−1.8900261
−3	1	−2.6667	−1.5417	−1.5416593
−3	2	−2.8822	−2.4462	−2.4436581
−3	4	−2.9583	−2.8415	−2.8412273

In Table 8, F_{max} is presented for various magnetic parameter m with $s = 0$ using Ariel's series solution (Section 3 [36]), the approximate solution (Section 6 [36]), Watanabe and Oyama solution [48] and the presented method with $N = 30$ and scaling factor $L = 3.5$. It is seen from this table that the maximum percentage of the absolute errors between the presented method, Ariel's series solution [36] and the approximate solution [36] is $4.94 \times 10^{-5}\%$ and $1.53 \times 10^{-1}\%$, respectively.

Table 8. Variation of F_{max} with magnetic parameter m for s = 0

m	Ariel [36]	Approximate [36]	Watanabe and Oyama [48]	Presented method
0	0.180767	0.165428	0.180000	0.1807671663
0.2	0.146361	0.135413	0.147925	0.1463606999
0.4	0.119254	0.111850	0.121887	0.1192540268
0.6	0.098537	0.093631	0.100841	0.0985367532
0.8	0.082842	0.079577	0.083943	0.0828418247
1	0.070873	0.068659	0.070514	0.0708725057
1.2	0.061608	0.060071	0.060015	0.0616084645
1.4	0.054309	0.053212	0.052025	0.0543094459
1.6	0.048454	0.047651	0.046224	0.0484540426
1.8	0.043676	0.043075	0.042378	0.0436763960
20	0.039718	0.039258	0.040333	0.0397175633
2.5	0.032303	0.032048	0.042732	0.0323025502
3	0.027170	0.027016	0.056676	0.0271702757
4	0.020572	0.020504	0.137292	0.0205722221
5	0.016532	0.016496	0.369746	0.0165317959
6	0.013810	0.013790	1.006518	0.0138104608
7	0.011855	0.011842	2.739247	0.0118552280
8	0.010383	0.010375	7.449955	0.0103834194
9	0.009236	0.009230	20.255232	0.0092358780
10	0.008316	0.008312	55.063673	0.0083162724

For the tangential direction, define the displacement thickness δ_{dis} as:

$$\delta_{dis} = \int_0^\infty G(\eta)d\eta \tag{76}$$

The momentum thickness for the flow about a rotating disk as defined by Stuart [49] is:

$$\delta_{mom} = \int_0^\infty G(\eta)(1 - G(\eta))d\eta \tag{77}$$

Table 9 shows the values of displacement thickness δ_{dis} and momentum thickness δ_{mom} obtained by Kumar et. al [35] and presented method with $N = 25$ and scaling factor $L = 9$ for some chosen values of s and m. Equations (76) and (77) include the numerous integrals. It is recommended to use the numerical integration rules such as Gauss Laguerre rule. The displacement thickness increases for decreased suction and decreases for decreased injection. For all values of injection, displacement thickness increases significantly with decreased m. The displacement thickness is slightly affected by increasing m when the suction value is larger, whereas the displacement thickness changes greatly with increases in m when the suction values become small. Similar trends are observed for momentum thickness.

Table 9. Effect of s and magnetic number m on displacement thickness δ_{dis} and momentum thickness δ_{mom}

s	m	δ_{dis}		δ_{mom}	
		Kumar et. al [35]	Presented method	Kumar et. al [35]	Presented method
2	0.1	0.47727	0.477268	0.23830	0.238298
2	0.5	0.44289	0.442893	0.22123	0.221229
2	1	0.41017	0.410166	0.20494	0.204942
2	2	0.36407	0.364075	0.18197	0.181966
2	4	0.30828	0.308284	0.15411	0.154113
1	0.1	0.78192	0.781922	0.38723	0.387225
1	0.5	0.68282	0.682821	0.33973	0.339725
1	1	0.59708	0.597084	0.29775	0.297749
1	2	0.49318	0.493181	0.24631	0.246311
1	4	0.38858	0.388578	0.19421	0.194210
0	0.1	1.2363	1.236254	0.58847	0.588466
0	0.5	1.0755	1.075465	0.52567	0.525667
0	1	0.89896	0.898964	0.44505	0.445046
0	2	0.68477	0.684770	0.34131	0.341311
0	4	0.49577	0.495767	0.24767	0.247674
−1	0.1	1.7252	1.725218	0.76046	0.760460
−1	0.5	1.5623	1.562257	0.73459	0.734551
−1	1	1.3048	1.304834	0.63569	0.635694
−1	2	0.94240	0.942396	0.46784	0.467836
−1	4	0.63162	0.631625	0.31531	0.315308
−2	0.1	2.2707	2.270674	0.91238	0.912377
−2	0.5	2.1129	2.112930	0.94692	0.946928
−2	1	1.7822	1.782588	0.85028	0.850624
−2	2	1.2534	1.253626	0.61869	0.618641
−2	4	0.79339	0.793426	0.39564	0.395670

For some selected values of Prandtl number (Pr) and s, Table 10 gives a comparison between the presented method with $N = 30$ and the results reported by Kumar et. al [35] for magnetic interaction number $m = 0.5$. It can be seen that the Nusselt number increases as suction increases but decreases as injection increases. This is due to the fact that increasing suction parameter lead to a thinner boundary layer thickness on the disk as was shown in Fig 2-a, which in turn results in an increase in heat transfer coefficient, Nu. For a given value of s, Nusselt number increases as Prandtl number increases. Similarly, for some values of magnetic interaction number m and Prandtl number (Pr). Table 11 gives a comparison between the presented method with $N = 30$ and the results reported by Kumar et. al [35] for uniform suction parameter $s = 1$. Here, we can see that the Nusselt number increases as magnetic number decreases. Decreasing magnetic number m leads to more incoming cold flow velocities ($-H(\eta)$) towards the rotating disk (See Figs 4b and 4c) and hence elevates the heat transfer rates. Furthermore, for a given m, Nusselt number increases as Prandtl number increases. It is observed from Tables 10 and 11 that the maximum percentage of the absolute errors between the presented method and the results obtained by Kumar et al. [35] is $1.50 \times 10^{-4}\%$ and $6.00 \times 10^{-3}\%$, respectively.

Figure 5 shows the logarithmic of absolute values of Chebyshev coefficients as computed for several scaling factor L. The optimum L for $N = 30$ is about $L = 8$, but is smaller for smaller N: note that the curves for small L are well below those of the solid circles for $L = 8$.

Table 10. Effect of Prandtl number (Pr) and s on Nusselt number $Nu = -\theta'(0)$ for $m = 0.5$

$s\backslash Pr$	Kumar et. al [35]			Presented method		
	0.1	1.0	10.0	$0.1(L = 7.304)$	$1.0(L = 9.200)$	$10.0(L = 1.500)$
4	0.4006091	4.002395	40.00112	0.4006091	4.0023950	40.0011209
3	0.3013329	3.005322	30.00255	0.3013329	3.0053220	30.0025492
2	0.2036261	2.015051	20.00770	0.2036261	2.0150512	20.0076992
1	0.1126061	1.059119	10.03991	0.1126066	1.0591194	10.0399115
0	0.0428310	0.2826559	0.9515366	0.0428302	0.2826559	0.9515363
-1	0.0031799	0.0034330	$----$	0.0031794	0.0034329	$----$

Table 11. Effect of m and Prandtl number (Pr) on Nusselt number $Nu = -\theta'(0)$ for $s = 1$

$m\backslash Pr$	Kumar et. al [35]			Presented method		
	0.1	1.0	10.0	$0.1(L = 7.600)$	$1.0(L = 7.600)$	$10.0(L = 1.500)$
0	0.1225589	1.0925388	10.054518	0.1225594	1.0925388	10.0545181
0.5	0.1126061	1.0591194	10.039911	0.1126067	1.0591194	10.0399115
1	0.1081711	1.0418339	10.031811	0.1081716	1.0418339	10.0318114
2	0.1044617	1.0254037	10.023168	0.1044619	1.0254037	10.0231684
3	0.1029297	1.0177857	10.018525	0.1029298	1.0177857	10.0185246
4	0.1021232	1.0134742	10.015565	0.1021232	1.0134742	10.0155645

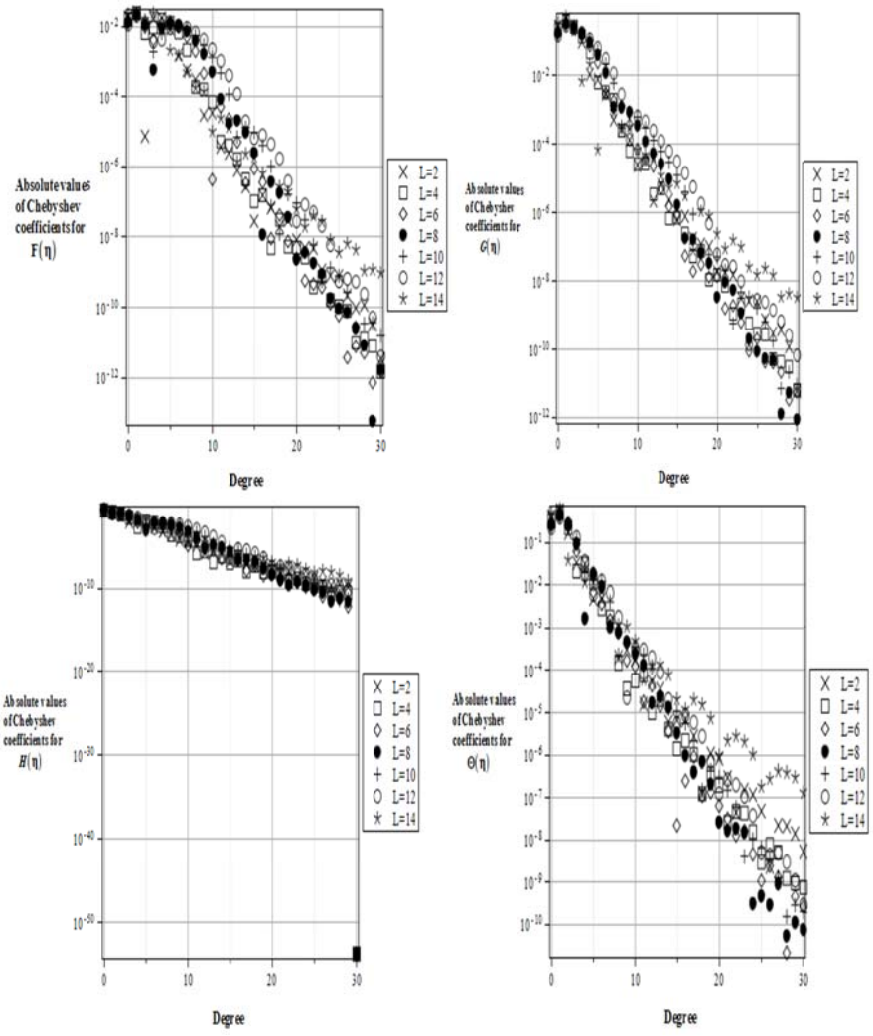

Fig. 5. The logarithmic of absolute values of Chebyshev coefficients $\tilde{f}_j, \tilde{g}_j, \tilde{h}_j$ and $\tilde{\theta}_j$ versus j for seven values of L. The solid circles show the best choice for $N = 30$, which is $L = 8$ when $m = 1, s = 2$ and $Pr = 2$

6. CONCLUSION

The aim of the this study is to develop an efficient and accurate numerical method based on pseudo-spectral collocation method and extrapolation for finding the approximate solutions of the system of nonlinear ordinary differential equations derived from similarity transform for the MHD flow about a rotating disk subject to a uniform suction and injection with heat transfer. The difficulty in this type of equation, due to the existence of its boundary condition in the infinity, is overcome here. Indeed, the method presented in this paper used a set of Chebyshev polynomials and solved this problem on the semi-infinite domain without truncating it to a finite domain. The comparisons are also made between the results of the presented method and other methods. It is found that the results of the present works agree well with other methods. The validity of this method is based on the assumption that it converges by increasing the number of collocation points. The present success of the proposed method for the nonlinear problem of MHD flow about a rotating disk subject to a uniform suction and injection verifies that the method is a useful tool for the solution of nonlinear problems in fluid mechanics.

Acknowledgements: The authors are very grateful to one of the referees for carefully reading this paper and for the comments and suggestions which have improved the paper.

REFERENCES

1. Smith, G. D. (1985). *Numerical solution of partial differential equations*. New York: Oxford University Press Inc.
2. Butcher, J. C. (2008). *Numerical methods for ordinary differential equations*. England: John Wiley and Sons Ltd.
3. Nath, Y., Prithviraju, M. & Mufti, A. A. (2006). Nonlinear static and dynamics of antisymmetric composite laminated square plates supported on nonlinear elastic subgrade. *Commun. Nonlinear. Sci. Numer. Simulat.*, Vol. 11, pp. 340-54.
4. Civalek, O. (2006). Harmonic differential quadrature-finite differences coupled approaches for geometrically nonlinear static and dynamic analysis of rectangular plates on elastic foundation. *J. Sound. Vibr*., Vol. 294, pp. 966-980.
5. Civalek, O. (2007). Nonlinear analysis of thin rectangular plates on Winkler-Pasternak elastic foundations by DSC-HDQ methods. *Appl. Math. Model*., Vol. 31, pp. 606-624.
6. Snyder, M. A. (1966). *Chebyshev methods in numerical approximation*. Englewood Cliffs, N.J: Prentice-Hall Inc.
7. Clenshaw, C. W. & Curtis, A. R. (1960). A method for numerical integration on an automatic computer. *Numer. Math.*, Vol. 2, pp. 197-205.
8. Boyd, J. P. (2001). *Chebyshev and fourier spectral methods*. Dover Publications Inc., Mineola, NY, 2nd edition.
9. Johnson, C. (1988). *Numerical solutions of partial differential equations by finite element method*. Cambridge: Cambridge University Press.
10. Karmishin, A. V., Zhukov, A. I. & Kolosov, V. G. (1990). *Methods of dynamics calculation and testing for thin-walled structures*. Moscow: Mashinostroyenie.
11. Lyapunov, A. M. (1992). *General problem on stability of motion* (English translation). London: Taylor and Francis.
12. Nayfeh, A. H. (1973). *Perturbation methods*. New York: Wiley Interscience.
13. Nayfeh, A. H. (1985). *Problems in perturbations*. NewYork: Wiley.
14. Adomian, G. (1994). *Solving frontier problems of physics: the decomposition method*. Dordrecht: Kluwer Academic Publishers.

15. He, J. H. (1999). Variational iteration method – a kind of non-linear analytical technique: some examples. *Int. J. Nonlinear. Mech*., Vol. 34, pp. 699-708.
16. He, J. H. (2000). Variational iteration method for autonomous ordinary differential systems. *Appl. Math. Comput*., Vol. 114, pp. 115-23.
17. He, J. H. (2003). Homotopy perturbation method: A new nonlinear analytical technique. *Appli. Math. Comput*., Vol. 135, pp. 73-79.
18. He, J. H. (2004). The homotopy perturbation method for nonlinear oscillators with discontinuities. *Appli. Math. Comput*., Vol. 151, pp. 287-292.
19. Liao, S. J. (2003). *Beyond perturbation: Introduction to the homotopy analysis method*. Hall/CRCPress, Boca Raton, FL, USA.
20. Xu, H., Liao, S. J. & Pop, I. (2006). Series solutions of unsteady boundary layer flow of a micropolar fluid near the forward stagnation point of a plane surface. *Acta. Mech*., Vol. 184, pp. 87-101.
21. Canuto, C., Hussaini, M., Quarteroni, A. & Zang, T. (1988). *Spectral methods in fluid dynamics*. Springer, Berlin.
22. Gottlieb, D. & Orszag, S. A. (1977). Numerical analysis of spectral methods: theory and applications. *CBMS-NSF Regional Conference Series, Applied Mathematics*, Vol. 26, SIAM, Philadelphia, PA.
23. Tifford, A. N. & Chu, S. T. (1952). On the flow around a rotating disk in a uniform stream. *Journal of Aeronautical Sciences*, Vol. 19, pp. 284-285.
24. Mehmood, A., Ali, A., Takhar, H. S., Beg, O. A., Islam, M. N. & Wilson L. S. (2010). Unsteady Von Karman swirling flow: analytical study using the Homotopy Method. *Int. J. Appl. Math. Mech*., Vol. 6, pp. 67-84.
25. Beg, O. A., Zueco, J. & Lopez-Ochoa, L. M. (2011). Network numerical analysis of optically-thick hydromagnetic slip flow from a porous spinning disk with radiation flux, variable thermophysical properties and surface injection effects. *Chemical Engineering Communications*, Vol. 198, pp. 360-384.
26. Ziael-Rad, S. (2005). Finite element model updating of rotating structures using different optimization techniques. *Iranian Journal of Science & Technology, Transaction B, Engineering*. Vol. 29, pp. 569-585.
27. Von Karman, T. (1921). Uber laminare and turbulente reibung. *ZAMM*., Vol. 1, pp. 233-252.
28. Cochran, W. G. (1934). The flow due to a rotating disk. *Proc. Camb. Phil. Soc*., Vol. 30, pp. 365-375.
29. Millsaps, K. & Polhausen, K. (1952). Heat transfer by laminar flow from a rotating plate. *J. Aero. Sci*., Vol. 19, pp. 120-126.
30. Stuart, J. T. (1954). On the effects of uniform suction on the steady flow due to a rotating disk. *Quart. J. Mech. Appl. Math*., Vol. 7, pp. 446-457.
31. Sparrow, E. M. & Gregg, J. L. (1959). Heat transfer from a rotating disk to fluids of any Prandtl number. *J. Heat Trans. ASME*., Vol. 81, pp. 249-251.
32. Benton, E. R. (1966). On the flow due to a rotating disk. *J. Fluid. Mech*., Vol. 24, pp. 781-800.
33. Kuiken, H. K. (1971). The effect of normal blowing on the flow near a rotating disk of infinite extent. *J. Fluid Mech*., Vol. 47, pp. 789-798.
34. Ackroyd, J. A. D. (1978). On the steady flow produced by a rotating disc with either surface suction or injection. *J. Eng. Math*., Vol. 12, pp. 207-220.
35. Kumar, S. K., Thacker, W. I. & Watson, L. T. (1988). Magnetohydrodynamic flow and heat transfer about a rotating disk with suction and injection at the disk surface. *Comput. Fluids*., Vol. 16, pp. 183-193.
36. Ariel, P. D. (2002). On computation of MHD flow near a rotating-disk. *Z. Angew. Math. Mech*., Vol. 82, pp. 235-246.
37. Turkyilmazoglu, M. (2010). Purely analytic solutions of magnetohydrodynamic swirling boundary layer flow over a porous rotating disk. *Comput. Fluids*., Vol. 39, pp. 793-799.
38. Turkyilmazoglu, M. (2011). Analytic approximate solutions of rotating disk boundary layer flow subject to a uniform vertical magnetic field. *Acta. Mech*., Vol. 218, pp. 237-245.

39. Sutton, G. W. & Sherman, A. (1965). *Engineering magnetohydrodynamics*. McGraw-Hill Book Co.
40. Attia, H. A. (2009). Steady flow over a rotating disk in porous medium with heat transfer. *Nonlinear Anal: Modell Control*., Vol. 14, pp. 21-26.
41. Millsaps, K. & Pohlhausen, K. (1952). Heat transfer by laminar flow from a rotating disk. *J. Aeronaut. Sci*., Vol. 19, pp. 120-126.
42. Tang, T. & Trummer, M. R. (1996). Boundary layer resolving pseudospectral methods for singular perturbation problems. *SIAM J. Sci. Comput*., Vol. 17, pp. 430-438.
43. Shen, J. & Wang, L. (2009). Some recent advances on spectral methods for unbounded domains. *Commun. Comput. Phys*., Vol. 5, pp. 195-241.
44. Boyd, J. P. (1982). The optimization of convergence for Chebyshev polynomial methods in an unbounded domain. *J. Comput. Phys*., Vol. 45, pp. 43-79.
45. Ortega, J. M. & Rheinboldt, W. G. (1970). *Iterative solution of nonlinear equations in several variables*. New York: Academic Press.
46. Kelley, C. T. (1995). *Iterative methods for linear and nonlinear equations*. Philadelphia, PA: SIAM.
47. Pande, G. S. (1972). On the effects of uniform high suction on the steady MDH flow due to a rotating disk. *Appl. Sci. Res*., Vol. 11, pp. 205-212.
48. Watanabe, T. & Oyama, T. (1991). Magnetohydrodynamic boundary layer flow over a rotating disk. *ZAMM*, Vol. 71, pp. 522-524.
49. Stuart, J. T. (1954). On the effects of uniform suction on the steady flow due to a rotating disk. *Q. Jl Mech. appl. Math*., Vol. 7, pp. 446-457.